

An Efficient Finite-Element Time-Domain Method via Hierarchical Matrix Algorithm for Electromagnetic Simulation

Ting Wan, Rushan Chen, Jianjian She, Dazhi Ding, and Zhenhong Fan

Department of Communication Engineering
Nanjing University of Science and Technology, Nanjing, 210094, China
billwanting@163.com

Abstract — An efficient finite-element time-domain (FETD) method based on the hierarchical (\mathcal{H} -) matrix algorithm is presented. The FETD method is on the basis of the second-order vector wave equation, obtained by eliminating one of the field variables from Maxwell's equations. The time-dependent formulation employs the Newmark-beta method which is known as an unconditional stable time-integration method. \mathcal{H} -matrix algorithm is introduced for the direct solution of a large sparse linear system at each time step, which is a serious handicap in conventional FETD method. \mathcal{H} -matrix algorithm provides a data-sparse way to approximate the LU triangular factors of the FETD system matrix. Using the \mathcal{H} -matrix arithmetic, the computational complexity and memory requirement of \mathcal{H} -LU decomposition can be significantly reduced to almost logarithmic-linear. Once the \mathcal{H} -LU factors are obtained, the FETD method can be computed very efficiently at each time step by the \mathcal{H} -matrix formatted forward and backward substitution (\mathcal{H} -FBS). Numerical examples are provided to illustrate the accuracy and efficiency of the proposed FETD method for the simulation of three-dimension (3D) electromagnetic problems.

Index Terms — Direct solution, finite-element time-domain (FETD) method, \mathcal{H} -matrix algorithm, reduced complexity.

I. INTRODUCTION

As one of the most efficient numerical methods for the electromagnetic simulation, the finite-element time-domain (FETD) method has been widely applied to the analysis of various

problems in the field of computational electromagnetics (CEM) recently. The FETD method holds the advantages of the finite element method (FEM) by combining the geometrical adaptability and material generality for modeling arbitrary shaped and inhomogeneously dielectric-filled objects. Moreover, it can also obtain a wideband response like the finite-difference time-domain (FDTD) method [1]. Therefore, a variety of FETD schemes have been developed during the past decades [2-11]. These schemes fall into two categories. The first scheme solves the time-dependent Maxwell's equations directly. The other scheme discretizes the second-order vector wave equation, known as the curl-curl equation, involving one of the field variables from the Maxwell's equations. It is similar to the traditional frequency-domain FEM in spatial discretization and can be made unconditionally stable by using the Newmark-beta method for the temporal discretization [7].

Due to the attractive advantage of the unconditionally stable scheme, the implicit methods are popularly used in the FETD to solve the second-order vector wave equation. However, the capability of an implicit scheme is highly limited since a large sparse linear system needs to be solved at each time step [12,13]. There are two categories of methods for the solution of this sparse linear system, i.e., iterative methods and direct methods. The iterative methods are widely used for large-scale problems due to their $O(N)$ computational complexity, with N being the matrix size [14, 15]. However, the iterative methods encounter two obstacles. One is the slow convergence rate when the FETD system matrix is

ill-conditioned, the other is the heavy redundant computational consumption for dealing with problems with multiple right-hand-side (RHS) vectors. These obstacles can be overcome by direct methods. However, the direct methods face the high computational complexity and memory requirement. Nonlinear complexity is familiar in electrodynamic field, even for existing state-of-the-art sparse matrix solvers. As reported in [16], the optimal complexity of the FEM-based direct solvers was shown to be $O(N^{1.5})$. This means that the direct methods will face a great challenge or even become impractical with the number of unknowns increasing.

In this paper, a direct method based on the hierarchical (\mathcal{H} -) matrix algorithm is proposed to yield an efficient FETD scheme with reduced complexity. \mathcal{H} -matrices have first been introduced in 1999 [17], and subsequently they were widely used for different applications [18,19]. \mathcal{H} -matrices provide an inexpensive but sufficiently accurate approximation to fully populated matrices arising from an integral operator or from the inverse of the finite element discretisation of an elliptic or hyperbolic partial differential operator [20-23]. These matrices are not sparse in the sense that there are only few non-zero entries, but they are *data-sparse* in the sense that these matrices are described by only a few data, that is, certain sub-blocks of these matrices can be described by low-rank approximations which are represented by a product of two low-rank matrices [24,25]. \mathcal{H} -matrix arithmetic allows the LU decomposition multiplication to be implemented with nearly optimal complexity $O(k^a N \log^b N)$ with appropriate parameters a, b and a blockwise rank k . The FETD system matrix is sparse and can be represented by an \mathcal{H} -matrix without approximation, while its LU-factors can be approximated in data-sparse representations by \mathcal{H} -matrices [26]. Based on this, in this paper, an efficient \mathcal{H} -LU decomposition algorithm is developed for solving the sparse linear system of the FETD with computational complexity and memory requirement being close to $O(N \log^2 N)$ and $O(N \log N)$ respectively. It should be noted that the \mathcal{H} -LU decomposition multiplication only needs to be performed once, and then the \mathcal{H} -LU-factors are stored and enter the subsequent FETD computation by the fast \mathcal{H} -

forward and backward substitutions (FBS) at each time step.

This paper is structured as follows: in Section II, the theory of the FETD method based on the second-order vector wave equation is outlined, along with the Newmark-beta method yielding an unconditional stable FETD scheme. Then, the \mathcal{H} -matrix algorithm is presented in detail for the efficient solution of the sparse linear FETD system in Section III. In Section IV, some numerical results are presented to demonstrate the performance of the resulting FETD method. Finally, conclusions are presented in Section V.

II. FETD FORMULATION WITH THE NEWMARK-BETA METHOD

In the FETD method, the whole computational domain is terminated by the anisotropic perfectly matched layer (PML) backed with perfect electric conductor (PEC) wall. From the Maxwell's equations in the anisotropic material, the curl-curl equation can be derived as follows

$$\nabla \times \frac{1}{\mu} ([\Lambda]^{-1} \cdot \nabla \times E) - \omega^2 \varepsilon [\Lambda] E = 0, \quad (1)$$

where $[\Lambda]$ is a diagonal matrix that describes the anisotropic permittivity and permeability of the PML region [27,28].

To get the FETD solution, the frequency-domain formulation is converted to the time-domain version by using the following relationships

$$j\omega \leftrightarrow \frac{\partial}{\partial t} \quad -\omega^2 \leftrightarrow \frac{\partial^2}{\partial t^2} \quad \frac{1}{j\omega} \leftrightarrow \int_0^t \quad \frac{-1}{\omega^2} \leftrightarrow \int_0^t \int_0^t \quad (2)$$

Then, the computational domain is discretized with tetrahedral elements [29] and the electric field is expressed in terms of the basis functions associated with the edges of each element as

$$E = \sum_{i=1}^N W_i e_i, \quad (3)$$

where N is the total number of the edges in an element, W_i is the vector basis function associated with edge i , and e_i is the unknown coefficient, which is the circulation of the electric field along the edge i . After the Galerkin testing, a weak form can be obtained as follows

$$[A]e + [B] \frac{de}{dt} + [C] \frac{d^2e}{dt^2} + [D]f + [E]g = 0, \quad (4)$$

where

$$\begin{aligned}
[A]_{ij} &= \iiint_V \frac{1}{\mu_r} \nabla \times W_i \cdot \nabla \times W_j + \\
&\quad \frac{\varepsilon \mu_0}{\varepsilon_0^2} ([J]^2 + 2[K]) W_i \cdot W_j dV \\
[B]_{ij} &= \iiint_V \frac{2\varepsilon \mu_0}{\varepsilon_0} [J] W_i \cdot W_j dV \\
[C]_{ij} &= \iiint_V \varepsilon \mu_0 W_i \cdot W_j dV \\
[D]_{ij} &= \iiint_V \frac{2}{\mu_r \varepsilon_0} [I] \nabla \times W_i \cdot \nabla \times W_j dV + \\
&\quad \iiint_V \frac{2\varepsilon \mu_0}{\varepsilon_0^3} [L] W_i \cdot W_j dV \\
[E]_{ij} &= \iiint_V \frac{1}{\mu_r \varepsilon_0^2} [I]^2 \nabla \times W_i \cdot \nabla \times W_j dV + \\
&\quad \iiint_V \frac{\varepsilon \mu_0}{\varepsilon_0^4} [K]^2 W_i^{(1)} \cdot W_j^{(1)} dV \\
f &= \int_t edt, \quad g = \iint_t edt. \quad (5)
\end{aligned}$$

$[I]$, $[J]$, $[K]$ and $[L]$ are PML-related matrices [30]. Using the Newmark-Beta formulation, (4) can be approximated as

$$\begin{aligned}
&\left([A]\beta + [B]\frac{1}{2\Delta t} + [C]\frac{1}{\Delta t^2} \right) e^{n+1} = \\
&[A]((2\beta - 1)e^n - \beta e^{n-1}) + [B]\frac{1}{2\Delta t} e^{n-1} + \\
&[C]\frac{1}{\Delta t^2} (2e^n - e^{n-1}) + \quad (6) \\
&[D](\beta f^{n+1} + (1 - 2\beta)f^n + \beta f^{n-1}) + \\
&[E](\beta g^{n+1} + (1 - 2\beta)g^n + \beta g^{n-1}) \\
&= 0
\end{aligned}$$

It has been proven that unconditional stability is achievable by choosing the interpolation parameter $\beta \geq 1/4$, and it is further shown that this choice of $\beta = 1/4$ minimizes the solution error [5]. Equation (6) can be simplified as

$$[M]e^{n+1} = [b], \quad (7)$$

where $[M]$ and $[b]$ denote the resultant system matrix and right-hand-side (RHS) vector, respectively. At each time step, the updating of the electric field requires solving equation (7). Obviously, $[M]$ keeps invariable while $[b]$ changes with the time steps. For such multi-RHS-

vector problem, direct solution is a good choice. Here, an \mathcal{H} -LU decomposition algorithm is introduced for the direct solution of (7). Although $[M]$ is sparse, its LU-factors are in general dense. However, \mathcal{H} -matrix algorithm provides a data-sparse way to compute and store the LU-factors of $[M]$ at a low cost. After the \mathcal{H} -LU decomposition, the update can be fast computed by \mathcal{H} -FBS as follows

$$e^{n+1} = U_{\mathcal{H}}^{-1} L_{\mathcal{H}}^{-1} b, \quad (8)$$

where $L_{\mathcal{H}}$ and $U_{\mathcal{H}}$ are the approximate LU-factors with \mathcal{H} -matrix representations.

III. \mathcal{H} -MATRIX ALGORITHM

\mathcal{H} -matrix algorithm can be applied to the FETD method in the following five steps: 1. Construct the cluster tree by a hierarchical partitioning of the set of edge-based basis functions. 2. Construct the block cluster tree from a given cluster tree using appropriate admissibility condition. 3. Generate the \mathcal{H} -matrix representation of the FETD system matrix $[M]$. 4. Compute the \mathcal{H} -LU decomposition in \mathcal{H} -matrix formatted arithmetic to obtain the \mathcal{H} -LU-factors. 5. Perform the \mathcal{H} -FBS to obtain the solution of (7) at each time step.

A. Construction of the cluster tree

Let $I = \{1, 2, \dots, N\}$ be a finite index set, which includes the indices of all edge-based basis functions W_i ($i=1, 2, \dots, N$) in the entire computational domain. Obviously, the FETD system matrix $[M]$ has the $I \times I$ matrix indices. The construction of an \mathcal{H} -matrix representation of $[M]$ starts from the construction of a cluster tree. A tree T_I satisfying the following conditions is called a *cluster tree* to I :

1. I is the root of T_I .
2. If $t \in T_I$ is a leaf, then $|t| \leq n_{\min}$, where $|t|$ denotes the number of elements in the set I and n_{\min} is a relatively small number which is predetermined.
3. If $t \in T_I$ is not a leaf, then t has two sons $t_1, t_2 \in T_I$, and $t = t_1 \cup t_2$.

The set of sons of $t \in T_I$ is denoted by $S(t)$, and $L(T_I)$ stands for the set of leaves of T_I .

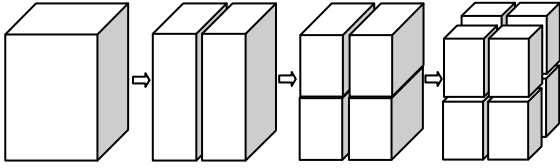


Fig. 1. Subdivision of a finite set using bounding boxes.

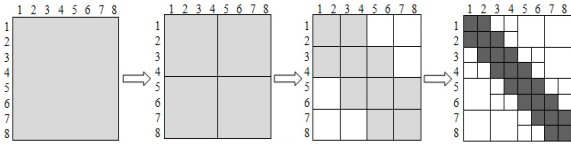


Fig. 3. Construction of a block cluster $T_{I \times I}$. Inadmissible blocks are *dark grey* and admissible blocks are *white*.

A cluster tree T_I is usually obtained by recursive subdivision of I . In this paper, binary trees are generated by subdividing an index set into two subsets recursively. This process continues until the size of the subset is smaller than a threshold parameter n_{\min} . n_{\min} is used to control the depth of the cluster tree, i.e., the maximum distance of a vertex to the root of the tree increased by one. In addition, $\Omega_t := \bigcup_{i \in t} \Omega_i$ is defined as the support of a cluster $t \in T_I$ where Ω_i is the support of the basis functions W_i . Ω_i can be chosen to be the bounding box B_i that comprises all the elements sharing W_i . A simple method for building a cluster tree is bisection based on geometry-based subdivisions of the index sets. Fig. 1 shows the process of bisection using bounding boxes and a simple example of a cluster tree is shown in Fig. 2.

B. Construction of the block cluster tree

A block cluster tree $T_{I \times I}$ arises from the grouping of pairs of clusters from the cluster tree T_I , as depicted in Fig. 3. $T_{I \times I}$ can be structured by recursively subdividing each block $v = t \times s$ ($t, s \in T_I$) into four disjoint subblocks $t_1 \times s_1$, $t_1 \times s_2$, $t_2 \times s_1$ and $t_2 \times s_2$ ($t_1, t_2 \in \mathcal{S}(t)$, $s_1, s_2 \in \mathcal{S}(s)$). This subdivision stops when

1. $|t| \leq n_{\min}$ or $|s| \leq n_{\min}$.
2. Clusters t and s satisfy admissibility condition.

The admissibility condition is a criterion for us to judge whether a block cluster $v \in T_{I \times I}$ allows for

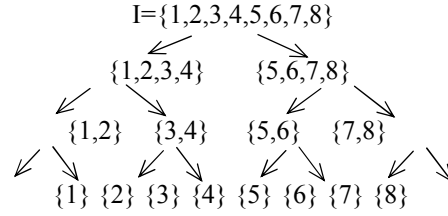


Fig. 2. A simple binary cluster tree T_I .

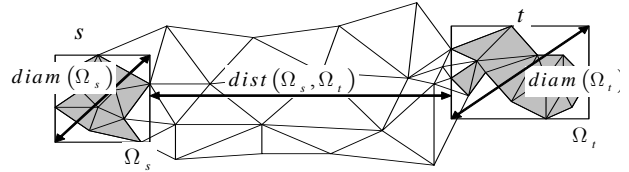


Fig. 4. Model graph of the admissibility condition.

a low-rank approximation. As shown in Fig. 4, a standard admissibility condition is given by

$$\max\{diam(B_t), diam(B_s)\} \leq \eta dist(B_t, B_s) \quad (9)$$

where B_t and B_s denote the minimal bounding box for the support of cluster t and s , $diam$ and $dist$ denote the Euclidean diameter and distance of cluster t and s respectively, and $\eta \in \mathbb{R}^+$ controls the trade-off. Blocks $v \in T_{I \times I}$ satisfying (9) are called admissible blocks, as shown in Fig. 3, which can be approximated by low-rank representation in the following Rk-matrices as follows

$$M|_{m \times n} = AB^T, A \in \mathbb{R}^{m \times k}, B \in \mathbb{R}^{n \times k}, \quad (10)$$

with A, B in full matrix representation, and k is much smaller than m and n .

C. Generate the \mathcal{H} -matrix representation of the FETD system matrix

Based on the block cluster tree $T_{I \times I}$, the class of \mathcal{H} -matrices with blockwise rank k and minimum block size n_{\min} of the FETD system matrix $[M]$ can be defined as

$$H(T, k) := \{M \in \mathbb{R}^{I \times I} \mid \forall t \times s \in L(T): \text{rank}(M|_{t \times s}) \leq k \text{ or } |t| \leq n_{\min} \text{ or } |s| \leq n_{\min}\}. \quad (11)$$

An \mathcal{H} -matrix induced by the block cluster tree $T_{I \times I}$ is on the basis of two cluster trees, named row cluster tree, and column cluster tree. In the \mathcal{H} -matrix structure of $[M]$ generated from the Galerkin method, the row and column cluster tree can be seen as the trees of the sets of original basis functions and testing basis functions respectively. Hence, all entries of $[M]$ can be filled into the

blocks of an \mathcal{H} -matrix compatibly. It should be pointed that, in the \mathcal{H} -matrix representation of $[M]$, all the nonzero matrix entries of $[M]$ are filled in inadmissible leaves while admissible leaves keep empty. This is because the partial differential operator is local, the nonzero entries of $[M]$ appear only in the case that the associated pair of bounding boxes B_i and B_s have a nonempty intersection. However, if the admissibility condition is satisfied, $dist(B_i, B_s)$ must be larger than zero since η is positive. Therefore, to generate the \mathcal{H} -matrix representation of $[M]$, one only needs to fill the inadmissible leaves with the nonzero entries of $[M]$ while keeps the admissible leaves empty. Inadmissible leaves are blocks stored as full matrices exactly so that $[M]$ can be represented by an \mathcal{H} -matrix without approximation.

D. \mathcal{H} -LU decomposition and \mathcal{H} -FBS

The obtained \mathcal{H} -matrix representation of the FETD system matrix $[M]$ has a structure of a quad tree based on a binary tree T_l . $[M]$ can be written as $M = \begin{bmatrix} M_{11} & M_{12} \\ M_{21} & M_{22} \end{bmatrix}$. The \mathcal{H} -LU decomposition can be computed recursively from this 2×2 block-matrix as follows

$$M = \begin{bmatrix} M_{11} & M_{12} \\ M_{21} & M_{22} \end{bmatrix} = \begin{bmatrix} L_{11} & \\ L_{21} & L_{22} \end{bmatrix} \begin{bmatrix} U_{11} & U_{12} \\ & U_{22} \end{bmatrix} \quad (12)$$

whose process can be expressed in detail as the following pseudo-code.

```

Procedure  $\mathcal{H}$ -LU decomposition ( $M, r, L, U$ )
if  $Son(r \times r) = \emptyset$  then
  calculate the LU decomposition  $M_{r \times r} = L_{r \times r} U_{r \times r}$ 
  exactly
else
  ( $Son(r) = \{r_1, r_2\}$ ,  $M = \begin{bmatrix} M_{11} & M_{12} \\ M_{21} & M_{22} \end{bmatrix}$ ,  $L = \begin{bmatrix} L_{11} & \\ L_{21} & L_{22} \end{bmatrix}$ ,
   $U = \begin{bmatrix} U_{11} & U_{12} \\ & U_{22} \end{bmatrix}$ )
  call  $\mathcal{H}$ -LU decomposition ( $M_{11}, r_1, L_{11}, U_{11}$ )
  call Block  $\mathcal{H}$ -Forward Substitution ( $L_{12}, M_{12}, r_1, r_2, U_{12}$ )
  call Block  $\mathcal{H}$ -Backward Substitution ( $U_{21}, M_{21}, r_2, r_1, L_{21}$ )

```

```

  call  $\mathcal{H}$ -LU decomposition ( $M_{22} - L_{21}U_{12}, r_2, L_{22}, U_{22}$ )
end

```

In the above procedure, a triangular solver $PX=Q$ or $XP=Q$ is required for a given lower or upper triangular matrix P and a given right-hand-side (RHS) matrix Q . The lower triangular solver can be viewed as a block \mathcal{H} -forward substitution recursively implemented as the following pseudo-code and the upper case as well as the block \mathcal{H} -backward substitution is similar. When X and Q are vector, the process of solving $PX=Q$ and $XP=Q$ is the \mathcal{H} -FBS.

```

Procedure Block  $\mathcal{H}$ -Forward Substitution ( $L, Q, r_i, r_j, X$ )
if  $Son(r_i \times r_j) = \emptyset$  then
  calculate the  $L_{\eta_i \times \eta_j} X_{\eta_i \times \eta_j} = Q_{\eta_i \times \eta_j}$  exactly
else
  ( $Son(r) = \{r_1, r_2\}$ ,  $L = \begin{bmatrix} L_{11} & \\ L_{21} & L_{22} \end{bmatrix}$ ,  $Q = \begin{bmatrix} Q_{11} & Q_{12} \\ Q_{21} & Q_{22} \end{bmatrix}$ ,
   $X = \begin{bmatrix} X_{11} & X_{12} \\ X_{21} & X_{22} \end{bmatrix}$ )
  call Block  $\mathcal{H}$ -Forward Substitution ( $L_{11}, Q_{11}, r_1, r_1, X_{11}$ )
  call Block  $\mathcal{H}$ -Forward Substitution ( $L_{11}, Q_{12}, r_1, r_2, X_{12}$ )
  call Block  $\mathcal{H}$ -Forward Substitution ( $L_{22}, Q_{21} - L_{21}X_{11}, r_2, r_1, X_{21}$ )
  call Block  $\mathcal{H}$ -Forward Substitution ( $L_{22}, Q_{22} - L_{21}X_{12}, r_2, r_2, X_{22}$ )
end

```

In all the procedures above, the exact addition and multiplication are replaced by the formatted \mathcal{H} -matrix counterparts (\oplus and \otimes). Truncation operator $\mathcal{I}_{k \leftarrow k}^{\mathcal{H}}$ based on truncated versions of the QR-decomposition and SVD is used to define \mathcal{H} -matrix addition $\mathcal{H}_1 \oplus \mathcal{H}_2 = \mathcal{I}_{k \leftarrow k}^{\mathcal{H}} (\mathcal{H}_1 + \mathcal{H}_2)$ and \mathcal{H} -matrix multiplication $\mathcal{H}_1 \otimes \mathcal{H}_2 = \mathcal{I}_{k \leftarrow k}^{\mathcal{H}} (\mathcal{H}_1 \times \mathcal{H}_2)$. In this paper, an adaptive truncation scheme with a relative truncation error $\varepsilon_{\mathcal{H}}$ is adopted, i.e., the rank of each admissible block is determined adaptively based on a required level of accuracy. The resulting \mathcal{H} -LU-factors $L_{\mathcal{H}}$ and $U_{\mathcal{H}}$ have the

Table 1: Performance of the \mathcal{H} -matrix algorithm

$\varepsilon_{\mathcal{H}}$	δ	\mathcal{H} -LU Time(s)	Memory(MB)	\mathcal{H} -FBS Time(s)
1.0e-1	1.39e-4	0.26	6.32	6.62e-3
1.0e-2	2.07e-5	0.36	8.69	7.88e-3
1.0e-3	1.12e-6	0.58	11.17	9.39e-3
1.0e-4	1.73e-8	0.84	14.64	1.08e-2
1.0e-5	2.29e-11	1.25	17.11	1.30e-2

same tree-structure as the \mathcal{H} -matrix representation of $[M]$, whereas the Rk-matrices may be not empty but filled with non-zero items during the recursion. The computational complexity of the \mathcal{H} -LU has been proven to be $O(k^2N\log^2N)$ [25] with blockwise rank k . Once $L_{\mathcal{H}}$ and $U_{\mathcal{H}}$ have been obtained, we only need to perform the \mathcal{H} -FBS as (8) at each time step of the FETD, whose computational complexity is $O(kN\log N)$.

IV. NUMERICAL RESULTS

In this section, some numerical examples of microwave circuits are simulated to demonstrate the performance of the proposed FETD method based on the \mathcal{H} -matrix algorithm. All computations are performed on an Intel Xeon E5405 workstation with 2.0GHz CPU and 16GB RAM in double precision.

A. A waveguide example

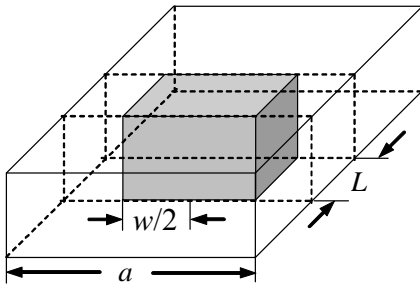


Fig. 5. Configuration of the full-height dielectric-filled rectangular waveguide.

The first example considers a waveguide filled with a full-height dielectric [31], as shown in Fig. 5. The rectangular waveguide has a width of $a=22.86\text{mm}$, and a height of $b=10.16\text{mm}$ and the inserted dielectric material slab has a dimension of

$w=12\text{mm}$ and $L=6\text{mm}$ and a relative permittivity of $\varepsilon_r=8.2$. In order to obtain an input reflection coefficient, two blocks of PML are placed at the input port and the out port to simulate the input and output matched loads. A modulated Gaussian pulse is applied, with mid-frequency $f_0=10.0\text{GHz}$ and bandwidth $=4.0\text{GHz}$. The \mathcal{H} -matrix algorithm associated parameter η in the admissibility condition (9) is set to be $\eta=1.0$ and the minimal block size is chosen as $n_{\min}=32$. First, the unknown number is fixed at $N=4,290$ to test the performance of the \mathcal{H} -LU decomposition for solving the FETD system. The relative error of the \mathcal{H} -LU factors $L_{\mathcal{H}}$ and $U_{\mathcal{H}}$ is defined as $\delta = \|I - U_{\mathcal{H}}^{-1}L_{\mathcal{H}}^{-1}M\| / \|I\|$, where I is identity matrix and $\|\cdot\|$ denotes 2-Norm. For different choices of the relative truncation error $\varepsilon_{\mathcal{H}}$, the relative error of $L_{\mathcal{H}}$ and $U_{\mathcal{H}}$, the time used for the \mathcal{H} -LU decomposition and the \mathcal{H} -FBS and the memory needed for the \mathcal{H} -LU decomposition are given in Table 1. Obviously, the relative error δ exponentially decreases with the $\varepsilon_{\mathcal{H}}$ decreasing, while the time and memory required for the \mathcal{H} -LU decomposition and the \mathcal{H} -FBS increase gradually. Fig. 6 shows the S parameter computed by the proposed \mathcal{H} -LU decomposition-based FETD method compared with that simulated by HFSS software in the case of $\varepsilon_{\mathcal{H}}=1.e-3$. Then, the relative truncation error is fixed $\varepsilon_{\mathcal{H}}=1.e-4$ and the unknown number increases from 19,317 to 609,364 by increasing the electric size of the waveguide to test the large-scale modeling capability. As shown in Figs. 7 and 8, the time complexity and the memory requirement can be observed to be very close to $O(N\log^2N)$ and $O(N\log N)$, respectively.

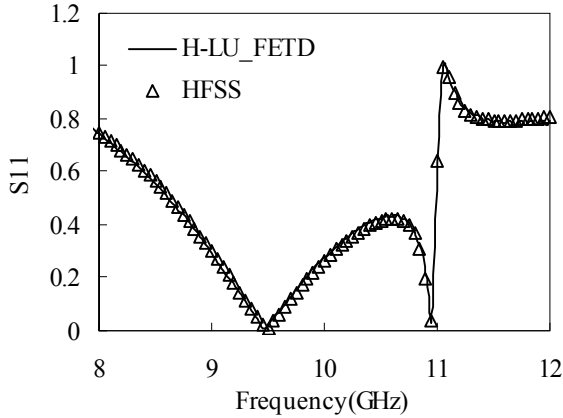


Fig. 6. S parameter of the waveguide filled with a full-height dielectric.

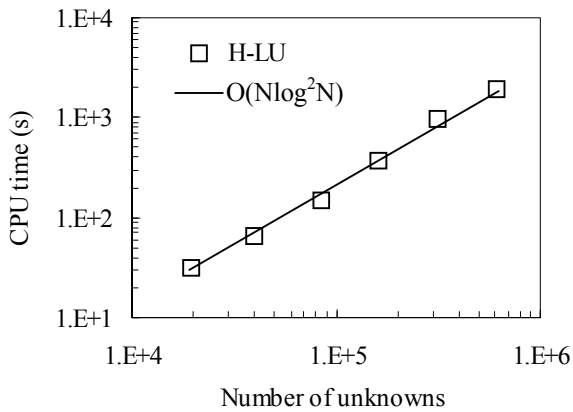


Fig. 7. Time required for the \mathcal{H} -LU decomposition.

B. A microstrip lowpass filter example

The second example deals with a microstrip lowpass filter. The detailed geometry of the metallization is shown in Fig. 9. The dielectric substrate has a thickness of $d = 0.76\text{mm}$ and a relative permittivity of $\epsilon_r = 2.43$.

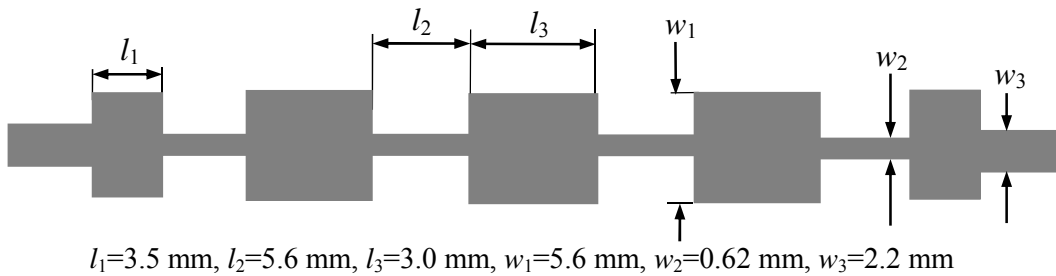


Fig. 9. Geometry and dimensions of the microstrip lowpass filter.

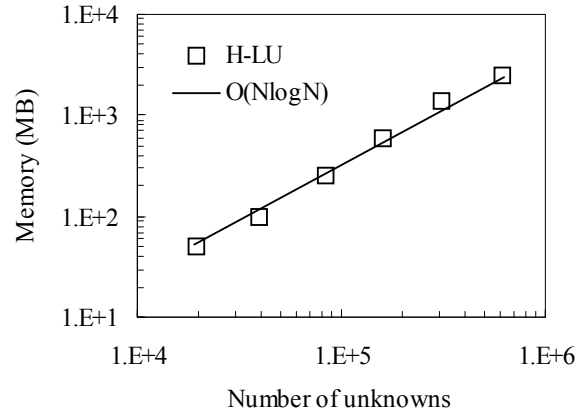


Fig. 8. Memory required for the \mathcal{H} -LU factors.

A modulated Gaussian pulse with mid-frequency $f_0 = 9.0\text{GHz}$ and bandwidth $= 16.0\text{GHz}$ is applied. The \mathcal{H} -matrix algorithm associated parameters are set to be $\eta = 1.0$, $n_{\min} = 64$. The relative truncation error is set to be $\epsilon_{\mathcal{H}} = 1.e - 4$. To test the performance of the \mathcal{H} -LU decomposition algorithm, the number of unknowns N increases from 42,927 to 412,863 by increasing the electric size of this microstrip. As shown in Figs. 10 and 11, the CPU time and memory requirements for the \mathcal{H} -LU are presented to be close to $O(N \log^2 N)$ and $O(N \log N)$, respectively. Moreover, the time requirements for the \mathcal{H} -FBS are also shown in Fig. 10, which are close to $O(N \log N)$. As can be seen from Fig. 10, even in the case $N = 231,263$, the computational time of the \mathcal{H} -FBS is only 3.15s, which means that once \mathcal{H} -LU factors are obtained, the computation of the FETD method at each time step can be finished with no more than 3.15s CPU time.

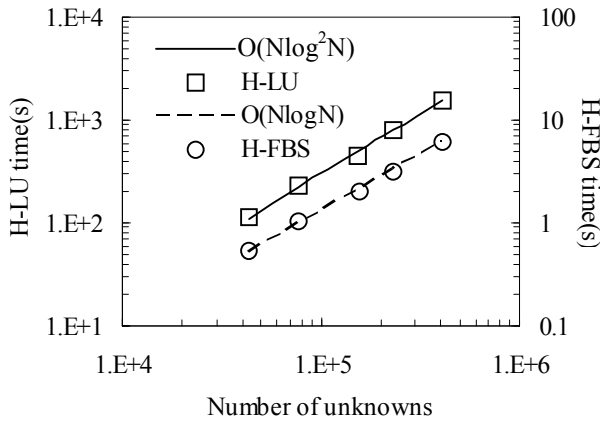


Fig. 10. Time required for the \mathcal{H} -LU decomposition and the \mathcal{H} -FBS.

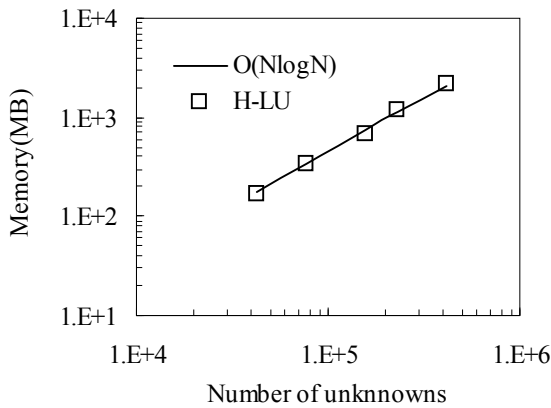


Fig. 11. Memory required for the \mathcal{H} -LU factors.

Meanwhile, good accuracy is achieved and the relative error is relatively stable as shown in Fig.

12, which is accurate enough for a correct solution. Figure 13 presents the S parameters computed by the \mathcal{H} -LU decomposition-based

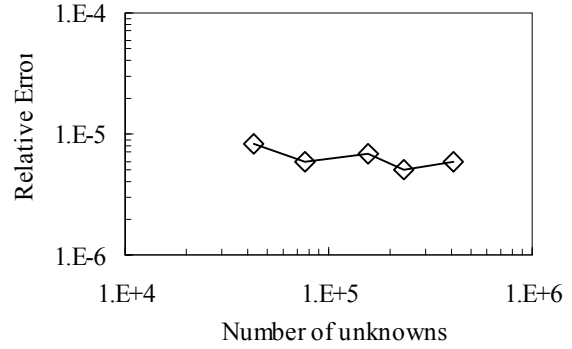


Fig. 12. Relative error of the \mathcal{H} -LU decomposition.

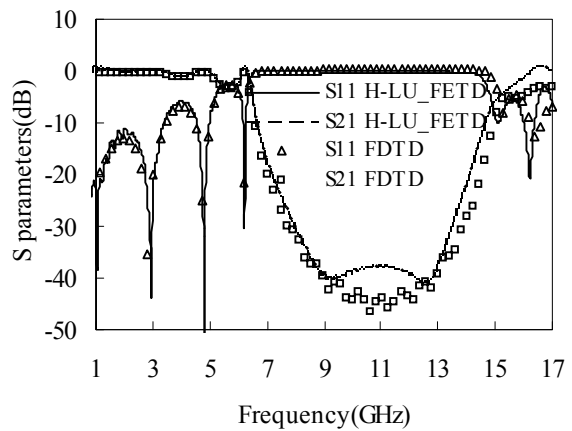
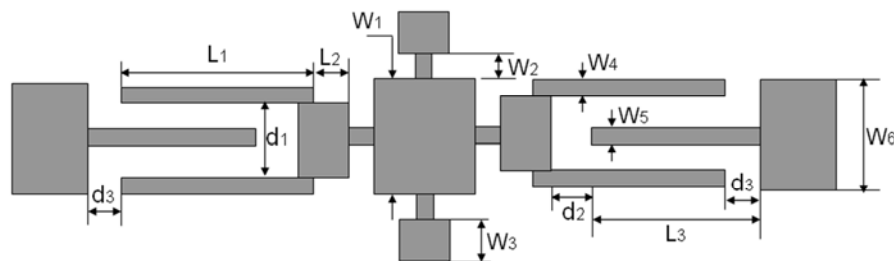


Fig. 13. S parameters of the microstrip lowpass filter.

FETD method in the case $N = 231,263$ compared with that computed by the finite-difference time-domain (FDTD) method.

C. A fractal-shaped UWB bandpass filter example

The last example deals with a fractal-shaped ultra-wideband (UWB) bandpass filter (BPF). Figure 14 shows the topology and detailed sizes of the UWB-BPF structure. The UWB-BPF has been



$$l_1=4.7 \text{ mm}, l_2=0.2 \text{ mm}, l_3=4.6 \text{ mm}, d_1=0.3 \text{ mm}, d_2=d_3=0.2 \text{ mm}, \\ w_1=1.3 \text{ mm}, w_2=w_4= w_5=0.1 \text{ mm}, w_3=0.3 \text{ mm}, w_6=0.76 \text{ mm}$$

Fig. 14. Geometry and dimensions of the fractal-shaped UWB bandpass filter.

fabricated on a substrate with relative permittivity $\epsilon_r = 2.43$ and thickness $d = 0.76\text{mm}$. A modulated Gaussian pulse with mid-frequency $f_0 = 7.0\text{GHz}$ and bandwidth $= 12.0\text{GHz}$ is applied. The total number of unknowns is 310,035. The \mathcal{H} -matrix algorithm associated parameters are set to be $\eta = 1.0$, $n_{\min} = 64$. Table 2 shows the relative error of $L_{\mathcal{H}}$ and $U_{\mathcal{H}}$, the time used for the \mathcal{H} -LU decomposition and the \mathcal{H} -FBS and the memory needed for the \mathcal{H} -LU decomposition with the relative truncation error $\epsilon_{\mathcal{H}}$ decreasing. Figure 15 presents the S parameters computed by the \mathcal{H} -LU decomposition-based FETD method in the case compared with that simulated by HFSS software. As can be seen from Fig. 15, reasonable agreement can be observed in the whole frequency band. The -10dB return loss bandwidth is from 3.2 GHz to 10.8GHz with mid-frequency 7.0GHz. What's more, in the bandwidth of interest, the designed UWB filter achieves an almost flat frequency response of insertion loss close to 0 dB.

V. CONCLUSION

In this paper, an efficient FETD method based on the second-order vector wave equation is generated by using the \mathcal{H} -matrix algorithm to directly solve the large sparse linear FETD system. The Newmark-beta scheme is implemented leading to an unconditionally stable FETD method. The \mathcal{H} -matrix algorithm provides a data-sparse way to compute and store the LU-factors of the FETD system matrix. This \mathcal{H} -LU decomposition can be implemented with reduced complexity, which highly improves the capability of the FETD method for large-scale modeling. Via the \mathcal{H} -FBS, the FETD system can be computed rapidly at each time step. Numerical results validate that the \mathcal{H} -LU-based direct solver significantly reduces the computational complexity and memory requirement to be close to $O(N\log^2 N)$ and $O(N\log N)$, respectively, and

Table 2: Performance of the \mathcal{H} -matrix algorithm

$\epsilon_{\mathcal{H}}$	δ	\mathcal{H} -LU Time(s)	Memory(MB)	\mathcal{H} -FBS Time(s)
1.0e-2	4.79e-3	626.2	783.5	3.6
1.0e-3	1.82e-4	854.8	1246.4	4.2
1.0e-4	2.77e-5	1387.5	1833.0	4.9

demonstrate the validity and efficiency of the proposed FETD method in the applications of electromagnetic simulation.

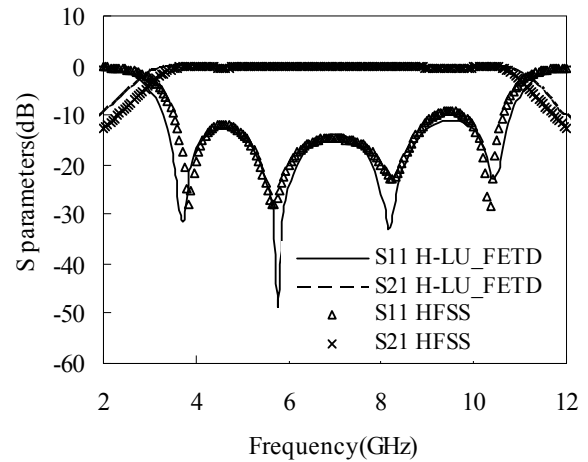


Fig. 15. S parameters of the fractal-shaped UWB bandpass filter.

ACKNOWLEDGMENT

We would like to thank the support of the Major State Basic Research Development Program of China (973 Program: 2009CB320201), Natural Science Foundation of 60871013, Jiangsu Natural Science Foundation of BK2009387 and NUST 2010ZYTS027.

REFERENCES

- [1] F. L. Teixeira, "A Summary Review on 25 Years of Progress and Future Challenges in FDTD and FETD Techniques," *Applied Computational Electromagnetic Society (ACES) Journal*, vol. 25, no. 1, pp. 1-14, Jan. 2010.
- [2] J. F. Lee, R. Lee, and A. C. Cangellaris, "Time-Domain Finite Element Methods," *IEEE Transactions on Antennas and Propagation*, vol. 45, pp. 430-442, 1997.

- [3] M. F. Wongm, O. Picon, and V. F. Hanna, "A Finite-Element Method Based on Whitney Forms to Solve Maxwell Equations in the Time-Domain," *IEEE Trans. Magn.*, vol. 31, pp. 1618-1621, 1995.
- [4] B. Donderici and F. L. Teixeira, "Mixed Finite-Element Time-Domain Method for Transient Maxwell Equations in Doubly Dispersive Media," *IEEE Trans. Microwave Theory Tech.*, vol. 56, no. 1, pp. 113-120, 2008.
- [5] H. -P. Tsai, Y. Wang, and T. Itoh, "An Unconditionally Stable Extended (USE) Finite-Element Time-Domain Solution of Active Nonlinear Microwave Circuits Using Perfectly Matched Layers," *IEEE Tran. Microwave Theory Tech.*, vol. 50, no. 10, pp. 2226-2232, Oct. 2002.
- [6] N. Marais and Davidson, "Numerical Evaluation of High-Order Finite Element Time Domain Formulations in Electromagnetics," *IEEE Trans. Antennas Propagat.*, vol. 56, vol. 12, pp. 3743-3751, 2008.
- [7] S. D. Gedney and U. Navsariwala, "An Unconditionally Stable Finite Element Time-Domain Solution of the Vector Wave Equation," *IEEE Tran. Microwave and Guided Wave Letters*, vol. 5, no. 10, pp. 332-334, Oct. 1995.
- [8] M. Feliziani and F. Maradei, "Hybrid Finite Element Solution of Time Dependent Maxwell's Curl Equations," *IEEE Trans. Magn.*, vol. 31, no. 3, pp. 1330-1335, May 1995.
- [9] R. N. Rieben, G. H. Rodrigue, and D. A. White, "A High-Order Mixed Vector Finite Element Method for Solving the Time Dependent Maxwell Equations on Unstructured Grids," *J. Comp. Phys.*, vol. 204, pp. 490-519, 2005.
- [10] S. D. Gedney, C. Luo, J. A. Roden, R. D. Crawford, B. Guernsey, J. A. Miller, T. Kramer, and E. W. Lucas, "The Discontinuous Galerkin Finite-Element Time-Domain Method Solution of Maxwell's Equation," *Applied Computational Electromagnetic Society (ACES) Journal*, vol. 24, no. 2, pp. 129-142, April 2009.
- [11] N. V. Kantartzis and T. D. Tsiboukis, *Modern EMC Analysis Techniques - Volume I: Time-Domain Computational Schemes*. San Rafael, CA, USA: Morgan & Claypool Publishers, 2008.
- [12] T. V. Yioultsis, N. V. Kantartzis, C. S. Antonopoulos, and T. D. Tsiboukis, "A Fully Explicit Whitney-Element Time-Domain Scheme with Higher Order Vector Finite Elements for Three-Dimensional High-Frequency Problems," *IEEE Trans. Magn.*, vol. 34, no. 5, pp. 3288-3291, Sept. 1998.
- [13] B. He and F. L. Teixeira, "A Sparse and Explicit FETD via Approximate Inverse Hodge (Mass) Matrix," *IEEE Microw. Wireless Comp. Lett.*, vol. 16, no. 6, pp. 348-350, 2006.
- [14] Y. Saad, *Iterative Methods for Sparse Linear Systems*. New York: PWS Publishing, 1996.
- [15] Z. Jia and B. Zhu, "A Power Sparse Approximate Inverse Preconditioning Procedure for Large Sparse Linear Systems," *Numer. Linear Algebra Appl.*, vol. 16, pp. 259-299, 2009.
- [16] A. George, "Nested Dissection of a Regular Finite Element Mesh," *SIAM J. on Numerical Analysis*, 10(2):345-363, April 1973.
- [17] W. Hackbusch, "A Sparse Matrix Arithmetic Based on \mathcal{H} -Matrices. I. Introduction to \mathcal{H} -Matrices," *Computing*, 62 (2):89-108, 1999.
- [18] W. Hackbusch and B. Khoromskij, "A Sparse \mathcal{H} -Matrix Arithmetic. Part II: Application to Multi-Dimensional Problems," *Computing*, 6, pp. 21-47, 2000.
- [19] S. Börm and L. Grasedyck, "Low-Rank Approximation of Integral Operators by Interpolation," *Computing*, vol. 72, pp. 325-332, 2004.
- [20] M. Bebendorf and S. Rjasanow, "Adaptive Low-Rank Approximation of Collocation Matrices," *Computing*, 70, pp. 1-24, 2003.
- [21] M. Bebendorf and W. Hackbusch, "Existence of \mathcal{H} -Matrix Approximants to the Inverse FE Matrix of Elliptic Operators with L^∞ -Coefficients," *Numer. Math.*, 95 (2003), pp.1-28.
- [22] H. Liu and D. Jiao, "A Direct Finite-Element-Based Solver of Significantly Reduced Complexity for Solving Large-Scale Electro-

- magnetic Problems,” IMS 2009, pp. 177-180, 2009.
- [23] H. Liu and D. Jiao, “Existence of \mathcal{H} -Matrix Representations of the Inverse Finite-Element Matrix of Electrodynamical Problems and \mathcal{H} -Based Fast Direct Finite-Element Solvers,” *IEEE Trans. on Microwave Theory and Techniques*, vol. 58, no. 12, pp. 3697-3709, Dec. 2010.
- [24] S. Borm, L. Grasedyck, and W. Hackbusch, “Induction to Hierarchical Matrices with Applications,” *Engineering Analysis with Boundary Elements*, no. 27, pp. 405-422, 2003.
- [25] L. Grasedyck and W. Hackbusch, “Construction and Arithmetics of \mathcal{H} -Matrices,” *Computing*, vol. 70, no. 4, pp. 295-344, August 2003.
- [26] M. Bebendorf, “Why Finite Element Discretizations can be Factored by Triangular Hierarchical Matrices,” *SIAM J. Matrix Anal. Appl.*, 45(4):1472-1494, 2007.
- [27] J. P. Berenger, “A Perfectly Matched Layer for the Absorption of Electromagnetic Waves,” *J. Compru. Phys.*, vol. 114, pp. 185-200, Oct. 1994.
- [28] S. D. Gedney, “An Anisotropic Perfectly Matched Layer-Absorbing Medium for the Truncation of FDTD Lattices,” *IEEE Transactions on Antennas and Propagation*, vol. 44, no. 11, pp. 1630-1639, 1996.
- [29] A. Bossavit, “Whitney Forms: A Class of Finite Elements for Three Dimensional Computations in Electromagnetism,” *IEE Proc. Pt. A*, vol. 135, no. 8, pp. 493-500, Nov. 1988.
- [30] Lei Du, R. S. Chen, and Z. B. Ye, “Perfectly Matched Layers Backed with the First Order Impedance Boundary Condition for the Time-Domain Finite-Element Solution of Waveguide Problems,” *Microwave and Optical Technology Letters*, vol. 50, no. 3, pp. 838-843, March 2008.
- [31] R. S. Chen, E. K. N. Yung, C. H. Chan, D. X. Wang, and D. G. Fang, “Application of the SSOR Preconditioned CG Algorithm to the Vector FEM for 3-D Full-Wave Analysis of Electromagnetic-Field Boundary-Value Pro-

blems,” *IEEE Trans. Microwave Theory Tech.*, vol. 50, no. 4, pp. 1165-1172, 2002.



Ting Wan was born in Huanggang, Hubei, China. He received the B.S. and M.S. degrees in Electrical Engineering from Nanjing University of Science and Technology (NJUST), Nanjing, China, in 2003 and 2006, respectively. He is currently working toward the Ph.D. degree in the Department of Communication Engineering at NJUST. His research interests include computational electromagnetics, antennas and microwave integrated circuits.



Rushan Chen was born in Jiangsu, China. He received his B.S. and M.S. degrees from the Dept. of Radio Engineering, Southeast University, in 1987 and in 1990, respectively, and his Ph.D. from the Dept. of Electronic Engineering, City University of Hong Kong in 2001. Since September 1996, he has been a Visiting Scholar with the Department of Electronic Engineering, City University of Hong Kong, first as Research Associate, then as a Senior Research Associate in July 1997, a Research Fellow in April 1998, and a Senior Research Fellow in 1999. From June to September 1999, he was also a Visiting Scholar at Montreal University, Canada. In September 1999, he was promoted to Full Professor and Associate Director of the Microwave & Communication Research Center in NJUST and in 2007, he was appointed Head of the Dept of Communication Engineering, Nanjing University of Science & Technology. His research interests mainly include microwave/millimeter-wave systems, measurements, antenna, RF-integrated circuits, and computational electro-magnetics. He is a Senior Member of the Chinese Institute of Electronics (CIE). He received the 1992 third-class science and technology advance prize given by the National Military Industry Department of China, the 1993 third class science and technology advance prize given by the National Education Committee of China, the 1996 second-class science and technology advance prize given by the

National Education Committee of China, and the 1999 first-class science and technology advance prize given by JiangSu Province as well as the 2001 second-class science and technology advance prize. At NUST, he was awarded the Excellent Honor Prize for academic achievement in 1994, 1996, 1997, 1999, 2000, 2001, 2002, and 2003. He has authored or co-authored more than 200 papers, including over 140 papers in international journals. He is the recipient of the Foundation for China Distinguished Young Investigators presented by the National Science Foundation (NSF) of China in 2003. In 2008, he became a Chang-Jiang Professor under the Cheung Kong Scholar Program awarded by the Ministry of Education, China.



Jianjian She was born in Jiangsu, China. He is currently working toward the M.S. degree in the Department of communication engineering at Nanjing University of Science and Technology, Nanjing, China. His research interests include computational electromagnetics, antennas and microwave integrated circuits.



Dazhi Ding was born in Jiangsu, China. He received the B.S. and Ph.D. degrees in Electromagnetic Field and Microwave Technique from Nanjing University of Science and Technology (NJUST), Nanjing, China, in 2002 and 2007, respectively. During 2005, he was with the Center of wireless Communication in the City University of Hong Kong, Kowloon, as a Research Assistant. He is currently a Lecturer with the Electronic Engineering of NJUST. He is the author or coauthor of over 20 technical papers. His current research interests include computational electromagnetics, electromagnetic scattering and radiation.



Zhenhong Fan was born in Jiangsu, China, in 1978. He received the M.Sc and Ph.D degrees in Electromagnetic Field and Microwave Technique from Nanjing University of Science and Technology (NJUST), Nan-jing, China, in 2003 and 2007, respectively. During 2006, he was with the Center of wireless Communication in the City University of Hong Kong, Kowloon, as a Research Assistant. He is currently a Lecturer with the Electronic Engineering of NJUST. He is the author or coauthor of over 20 technical papers. His current research interests include computational electromagnetics, electromagnetic scattering, and radiation.